Research Paper

Hyperbranched Polymer Integrated Membrane for the Removal of Arsenic(III) in Water

D.E. Vlotman [1], J.C. Ngila [1], T. Ndlovu [2], S.P. Malinga [1,*]

[1] Department of Applied Chemistry, University of Johannesburg, P.O. Box 17011, Doornfontein, 2028, South Africa
[2] Department of Chemistry, University of Swaziland, Private Bag 4, Kwaluseni, Swaziland

Article info

Keywords

Graphical abstract

Highlights

- HPEI-PSf membranes were evaluated for the removal of As(III).
- HPEI had an impact in hydrophilicity, water uptake and surface morphology.
- Three proposed removal mechanisms of As(III) are suggested.

Abstract

This work demonstrates the synthesis, characterization and application of a hyperbranched polyethyleneimine/polysulfone (HPEI/PSf) thin film composite (TFC) membrane. The membrane was accessed via an interfacial polymerization of trimesoyl chloride and HPEI. The membrane samples were characterized by Fourier Transform Infrared-Attenuated Total Reflectance (FTIR-ATR) spectroscopy, Scanning Electron Microscopy (SEM) and Atomic Force Microscopy (AFM). Contact angle and streaming potential measurements were used to measure the wettability and study the surface chemistry of the TFC membranes, respectively. Water flux and rejection studies were performed using a dead-end filtration cell system operated at 600 kPa. The binding affinity of the fabricated membranes to abstract As(III) from synthetic and spiked tap water samples was assessed. FTIR-ATR spectra illustrated that a polyamide film was successfully deposited onto the commercial PSf membrane. AFM analysis revealed that the surface roughness of the membranes increased from 13.9 nm to 140.0 nm upon HPEI loading. Contact angle measurements indicated an increase in the hydrophilicity from 86.95° for pristine PSf to 39.97° for the HPEI modified membranes. Generally, the HPEI/PSf membranes showed a high water uptake (up to 96.6±0.76%) as compared to the pristine PSf membranes (up to 53.5±0.7%). The hyperbranched polymer integrated membranes exhibited high As(III) retention of 78% and 55% for synthetic water and spiked tap water samples, respectively.

1. Introduction

Arsenic is a here naturally occurring metalloid, which is widely distributed throughout the environment (i.e. in air, water and soil). Industrial applications of arsenic include using it as alloying agent and in the preparation and processing of various materials such as glass, pigments, textiles, paper, metal adhesives, wood preservatives, pesticides, feed additives and pharmaceutical products. Whilst some industries use arsenic in the preparation and processing of these materials, others produce arsenic as a waste product.

Arsenic pollution has become one of the world's leading environmental challenges to the extent that arsenic was reported to be among the world's top six pollutants in 2010 [1]. The greatest threat to public health from arsenic originates from contaminated surface- and ground-water sources, which ultimately spill over and contaminate drinking water. Adverse health effects of arsenic on animals and humans include the alteration of the respiratory,

---
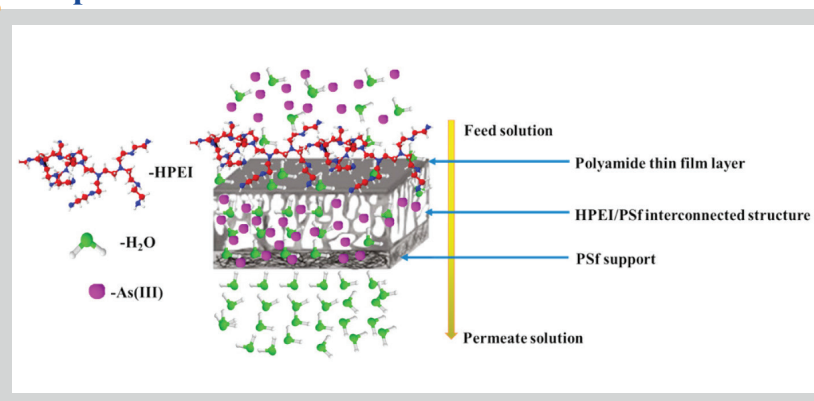
gastrointestinal, cardiovascular, nervous and hematopoietic systems [2].

South Africa is famous for its abundance of mineral resources and is a world leader in mining. Since arsenic is generally found in high concentrations near mining operation zones, it is not surprising that arsenic pollution originates primarily from mining activities in South Africa. Smelting, an industrial process that separates metals from their ore, can also produce a gaseous form of arsenic that ends up being released into the environment. To this end, arsenic-contaminated wastewater is often a by-product of South African smelting operations.

Although the South African National Standard (SANS) limits arsenic intake to 10 µg/L [3], high levels of arsenic are prevalent in certain parts of the country. For example, arsenic at levels of up to 100 µg/L were detected in the Springbok River, South Africa [4]. In another study, a sampling campaign involving 1514 South African boreholes revealed that boreholes in the Western Cape (Malmesbury) and North West (Potchefstroom) provinces of the country contained arsenic concentration levels as high as 10 mg/L and 7 mg/L, respectively [5].

Diverse technologies such as coagulation-flocculation, ion exchange, adsorption and membrane filtration have been used for the removal of heavy metals from water and wastewater [6]. Although they have been widely touted for their simplicity and effectiveness, these methods are limited by, among other things, their inability to completely remove As(III) from water systems [6, 7]. Of the known conventional treatment technologies, adsorption and membrane filtration technologies have been found to be reliable in the removal of both organic and inorganic pollutants from water [8–10]. For example, loose membranes have been successfully employed in the fractionation of direct dyes and salt solutions in textile industries [11–13]. An in-depth physical and chemical characterization of superhydrophillic loose poly(piperazineamide) based nanofiltration (NF) membranes (Sepro NF 6 and 2A, Ultura) was undertaken [14]. Whereas the Sepro NF 6 membrane was found to exhibit a salt (NaCl) transmission of 88%, the Sepro NF 2A membrane displayed a salt (NaCl) transmission of 67.3% (with an initial NaCl concentration of 0.01 mol L^{-1} for both membranes). The difference in salt rejection was attributed to the difference in the pore sizes of the membranes (Sepro NF 6: 0.64±0.03 nm; Sepro NF 2A: 0.52±0.01 nm). It was concluded that the Donnan's effect of the Sepro NF 6 were effectively weakened by the larger pore size of this membrane, and this ultimately resulted in greater salt transmission. The specific characteristics of these loose membranes augurs well for their application in the fractionation of organic solutes/salt aqueous systems.

The application of membrane technology for environmental remediation have several advantages, one of which is its potential to be coupled with adsorption-based techniques [15, 16]. To enhance the general performance of membranes, a new class of membranes can be synthesized by combining polymeric materials such as polyethersulfone (PES), polysulfone (PSf) or polyvinylidene fluoride (PVDF) with amphiphilic hyperbranched polymers [17]. These hyperbranched polymer matrix composite membranes exhibit superior performance over commercial membranes such as increased adsorption capacity, higher selectivity and enhanced stability [18].

Hyperbranched polyethyleneimine (HPEI) is a three-dimensional functional macromolecule, which consists of an interior diaminoethane core, interior branching ethyleneimine units and peripheral functional amine (NH$_2$) groups [19]. Other than their polydispersity characteristics, these polymers are asymmetrical in terms of their branching and structure [20]. Since HPEI has metal chelating properties, any functionalisation of porous commercial membranes with HPEI typically leads to a material that is capable of extracting heavy metals from aqueous solutions contaminated with metal pollutants [13, 14].

The metal chelating properties of the HPEI are attributable primarily to the internal amine functional groups, which have the ability to act as ligands and thus enable the complexation of various metals such as Cu, Fe and Ni [21-23]. HPEI can also induce hydrophilicity due to its abundant peripheral amine groups [24]. Increased hydrophilicity in membranes has been found to increase the pure water flux of the membrane. Results of research conducted on the effect of HPEI on the permeability and selectivity of PES membranes seem to indicate that both the density and thickness of the thin film layer on the membrane increases with the varied addition of HPEI [25]. At a concentration loading of 0.3% HPEI, the pure water flux was found to reach a maximum of 359.0 L·m^{-2}·h^{-1} at 0.1 MPa. It is worth quoting that the achieved pure water flux is 36 times higher than that of the pure PES membrane [25]. The rejection of bovine serum albumin (BSA) was found to be relatively high (96.1%) HPEI loading of 0.3%. However, the pure water flux was found to be inversely proportional to the rejection of BSA at HPEI concentration loading higher than 0.3%. An increase in the HPEI content (0.9% HPEI) resulted in a decrease in the pure water flux (from 359.0 L·m^{-2}·h^{-1} to 182.0 L·m^{-2}·h^{-1}) and an increase in the BSA rejection (from 96.1% to 97.1%). This therefore suggests that the permeability and selectivity of the membrane can simply be altered by adjusting the content of HPEI.

Various studies have been conducted on the application of membrane technology in the removal of As(III). For instance, Qu and co-workers studied the removal of arsenic [As(III) and As(V)] using direct contact membrane distillation on a PVDF membrane. In this study, the fabricated membrane was found to possess a high rejection of inorganic anions and cations; the rejection was independent of the solution pH and temperature [26]. The removal of both As(III) and As(V) were below the maximum concentration limit of 10 µg/L until the feed solution of As(III) and As(V) increased to 40 mg/L and 2000 mg/L, respectively. The morphology of the membranes, however, changed after the experiments, and this ultimately hinders their long-term performance and reuse [26]. The preparation and application of hyperbranched poly(amidoamine) [HPAMAM]-grafted poly(tetrafluoroethylene) [PTFE] microfiltration membranes in the removal of copper was demonstrated by Yoo and co-workers. The membranes were fabricated by surface amination of PTFE membranes with hydrazine and subsequently chemically coupled with the hydrophilic chelating agent HPAMAM. These membranes were found to adsorbed 1.42 g/m^2 Cu^{2+} ions from aqueous solutions and 90% desorption was achieved under acidic conditions. To this end, the adsorption capacity of the membranes towards Cu^{2+} was preserved after repeated reuse cycles [27]. The removal of Ni(II), Cu(II), Fe(III) and Cr(III) using a thin film composite polyamide membrane modified by UV-photo-induced grafting of poly(ethylene glycol) and acrylic acid was studied by Hong and co-workers. The rejection rates of most of these model metals pollutants were higher than 80%. The authors speculated that the rejection of the heavy metals was mainly due to an increased compaction of the membranes after surface grafting with PEG and acrylic acid. However, the build-up of metal ions on the membrane surface was found to be limiting factor, which diminished the life-span of the membranes [28].

The advantages of incorporating hyperbranched polymers on membrane substrates have clearly been demonstrated in several of the studies quoted above. It is noteworthy that most of these studies focused on the removal of As(III) and other heavy metals in simulated water. Moreover, studies involving the removal of arsenic using hyperbranched polymers were largely more successful in the removal of As(V) than As(III); which happens to be more soluble in water than the former. In this study, a hyperbranched polyethyleneimine modified ultrafiltration polysulfone (HPEI/PSf) membrane was fabricated and characterized using FTIR-ATR, SEM, AFM and contact angle measurements. The membranes were used for the removal of As(III) from synthetic and spiked tap water samples. As opposed to synthetic water samples where real water samples have been prepared by spiking water with a known model pollutant, in this paper, spiked tap water samples refers to tap water samples spiked with a model pollutant.

2. Experimental

2.1. Materials

A commercially available (MICRODYN-NADIR) porous polysulfone (RM US100 P1016) membrane with a cut-off weight of 100 kD was purchased from Memcon. Hyperbranched polyethyleneimine (HPEI, MW = 25,000 g/mol, with a 1°:2°:3° amine ratio of 34:40:26, respectively), was purchased from BASF. Analytical grade trimesoyl chloride (TMC) and *n*-hexane were purchased from Sigma-Aldrich and used as received. A reagent grade arsenic trioxide standard solution was prepared by appropriate dilutions of a 1000 µg/L stock solution (Sigma-Aldrich) before use.

2.2. Preparation of thin film composite PSf supported membranes

The membranes were prepared using an interfacial polymerization method [29]. Aqueous solutions were prepared by dissolving HPEI (1%, 2%, 3% and 4% w/v) in a 90/10 water/ethanol mixture. The commercial PSf membranes were then immersed in the aqueous solutions for 6 h at room temperature. Subsequently, the membranes were immersed for 2 min in a trimesoyl chloride (TMC) solution (0.2% w/v) in n-hexane. A roller was used to ensure uniform coating onto the membrane during the interfacial polymerization reaction. The modified membranes were then dried for 15 min at 60°C to allow further crosslinking of the polymeric membrane to occur.

2.3. Water uptake measurements

The water uptake of the separate separation active layer was determined by measuring the difference in weight between dry and wet membranes. The membranes were immersed in distilled water for 24 h followed by drying at 60°C for 24 h. Water uptake measurements were calculated according to Eq.

(1) [30]:

$$Water\ uptake\ (\%) = \frac{W_w - W_d}{W_d} \times 100 \qquad (1)$$

where W_w and W_d correspond to the weight of the wet and dry membranes, respectively.

2.4. Membrane characterization

The structural changes of the membranes were observed using Fourier Transform-Infrared-Attenuated Total Reflectance spectroscopy (FTIR-ATR), (Perkin Elmer, Spectrum 100).

Water contact angle measurements were used to quantify the degree of hydrophilicity prior to and after modification with HPEI and were recorded using a DataPhysics Optical Contact Angle (OCA) 15 EC equipped with video capture at room temperature. Drops (5 µL) of distilled water were deposited onto the membrane surface and the direct microscopic measurement of the contact angles was carried out with the goniometer.

After coating with carbon, the surface morphologies and cross section (frozen and fractured in liquid nitrogen) of the pristine PSf and modified membranes were observed under SEM (Joel, JSM 7500F). Atomic Force Microscopy (Veeco Di3100) was utilized to quantify changes in the topography of the pristine and modified membranes. The surface roughness (R_q) parameters of the membranes, expressed in terms of the mean roughness (R_a), were calculated from AFM images by Nanoscope V530r3sr3 software at scan areas of 5 µm × 5 µm.

2.5. Streaming potential studies

The membrane surface charge was determined using a SurPASS Electrokinetic Analyzer (Anton Paar GmbH, Graz, Austria). An aqueous solution of analytical grade KCl (10 mM) was used as the electrolyte solution, and 600 mL was used for each experimental run. Analyses were performed using an adjustable gap cell, which accommodates small planar samples with a rectangular size of 20 mm × 10 mm. The samples were firmly attached onto two sample holder blocks using double-sided adhesive tape. Streaming current and potential were measured using a standard program in the system using the following steps: a) rinsing with the electrolyte solution at 300 mbar for 180 seconds; b) performing flow check at 400 mbar for 120 seconds; and finally, c) determining streaming potential at 400 mbar for 180 seconds. Measurements were performed at the ambient pH of the solutions of about 5.8. The system was rinsed with Milli-Q water after every experimental run.

2.6. Porosity and membrane thickness

The porosity (ε) of the membranes was determined using Eq. (2) [31]:

$$\varepsilon = \frac{W_w - W_d}{Al d_w} \qquad (2)$$

where W_w and W_a are the weights of the wet and dry membranes, respectively. A is the membrane effective area (m^2), d_w is the density of distilled water (0.998 g/cm^3 at 20°C) and l is the membrane thickness (m). The thickness of the membranes was measured using ImageJ software.

The mean pore radius (r_m) of the synthesized membranes was calculated using the Guerout-Elfrord-Ferry equation, Eq. (3) [32]:

$$r_m = \sqrt{\frac{(2.9 - 1.75\varepsilon) \times 8\eta l Q}{\varepsilon A \Delta P}} \qquad (3)$$

where, η is the viscosity of water (8.9 × 10^{-4} Pas), Q is the volume of pure permeated water per unit time (m^3/s) and ΔP is the operating pressure (400 kPa).

2.7. Filtration studies

The pure water flux, permeate flux and rejection studies of the membranes were investigated using a dead-end filtration cell (Sterlitech stirred cell, HP4750). The feed side of the cell was pressured by nitrogen gas. The membranes were initially pressurized at 450 kPa transmembrane pressure until a steady flux was obtained. Six different pressures were used for the pure water flux measurements namely: 150, 200, 250, 300, 400 and 600 kPa.

The flux (J_w) was calculated using Eq. (4) [33]:

$$J_w = \frac{V}{A \Delta t} \qquad (4)$$

where J_w is the flux (L·m^{-2}·h^{-1}), V is the volume of distilled water (L), A is the effective area of the membrane (0.00146 m^2) and Δt is the time (h) taken to collect the permeate volume.

Synthetic and spiked tap water samples were prepared by diluting the 1000 µg/L arsenic trioxide (in 2% nitric acid) stock solution to 200 µg/L As(III) with distilled water and tap water, respectively. As(III) rejection studies were undertaken using a dead-end filtration cell under constant magnetic stirring. A feed solution of 200 µg/L As(III) (300 mL) was passed through the cell at 600 kPa transmembrane pressure. The concentration of the solute was measured using Inductively Coupled Plasma Optical Emission spectrometry (ICP-OES), ThermoFisher Scientific (ICAP 6500 duo). The observed rejection (%R) was calculated using Eq. (5) [34]:

$$\%R = \frac{C_f - C_p}{C_f} \times 100 \qquad (5)$$

where C_p denotes As(III) concentration in the permeate and C_f denotes As(III) concentration in the feed (µg/L).
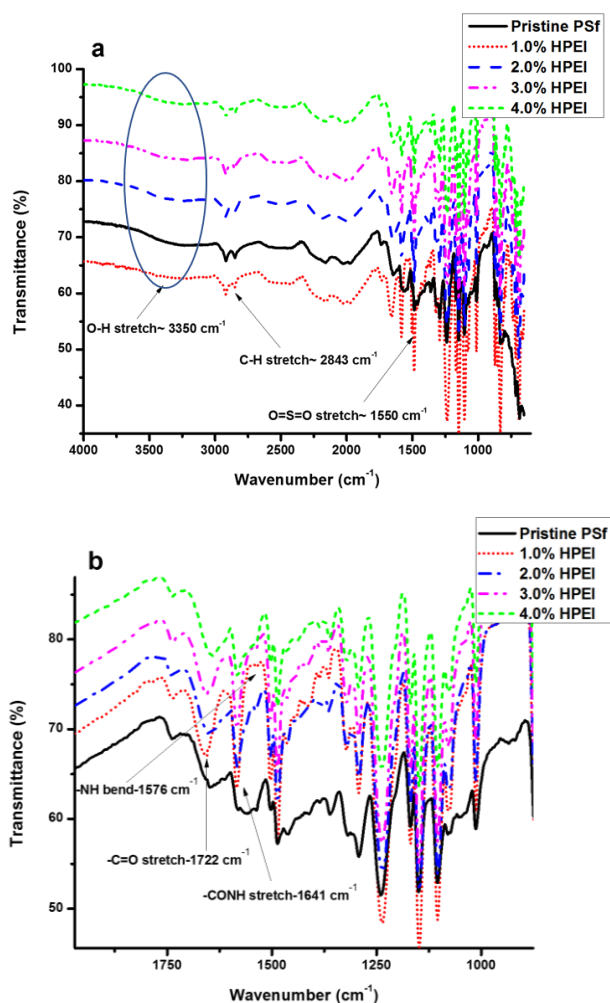

Fig. 1. (a) FTIR spectrum of pristine PSf and HPEI modified PSf membranes, (b) FTIR expansion of amide region.

3. Results and discussion

3.1. FTIR-ATR analysis

As illustrated in Figure 1 (a) and (b), the structural modification of the pristine PSf membrane was confirmed by FTIR-ATR analysis. Absorption
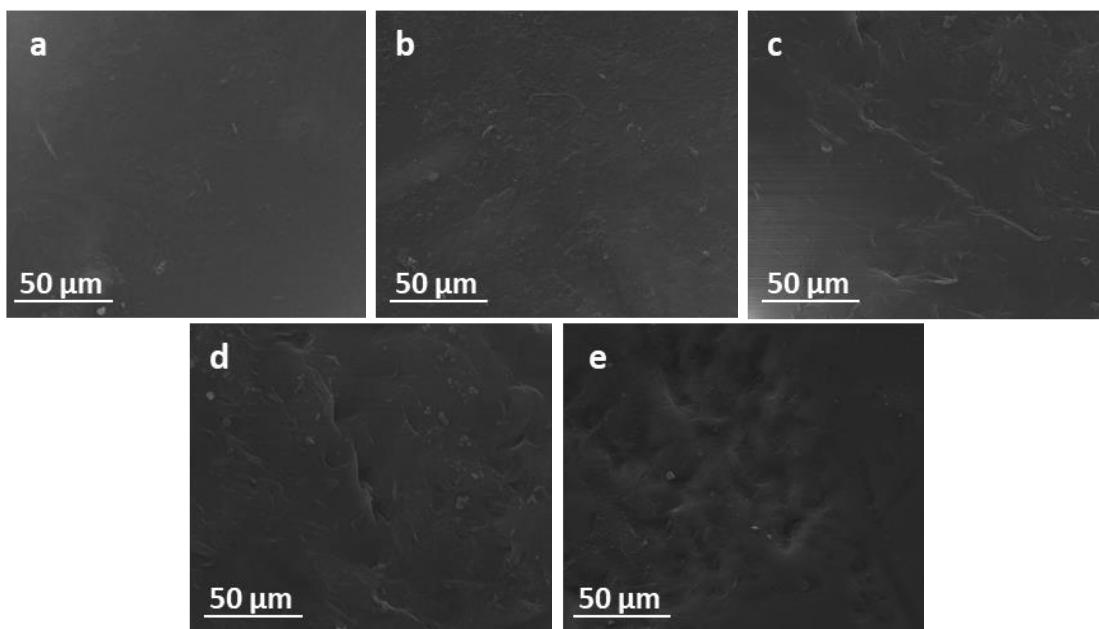
Fig. 2. Surface SEM images of (a) pristine PSf, (b) 1% HPEI/PSf, (c) 2% HPEI/PSf, (d) 3% HPEI/PSf, and (e) 4% HPEI/PSf membranes.
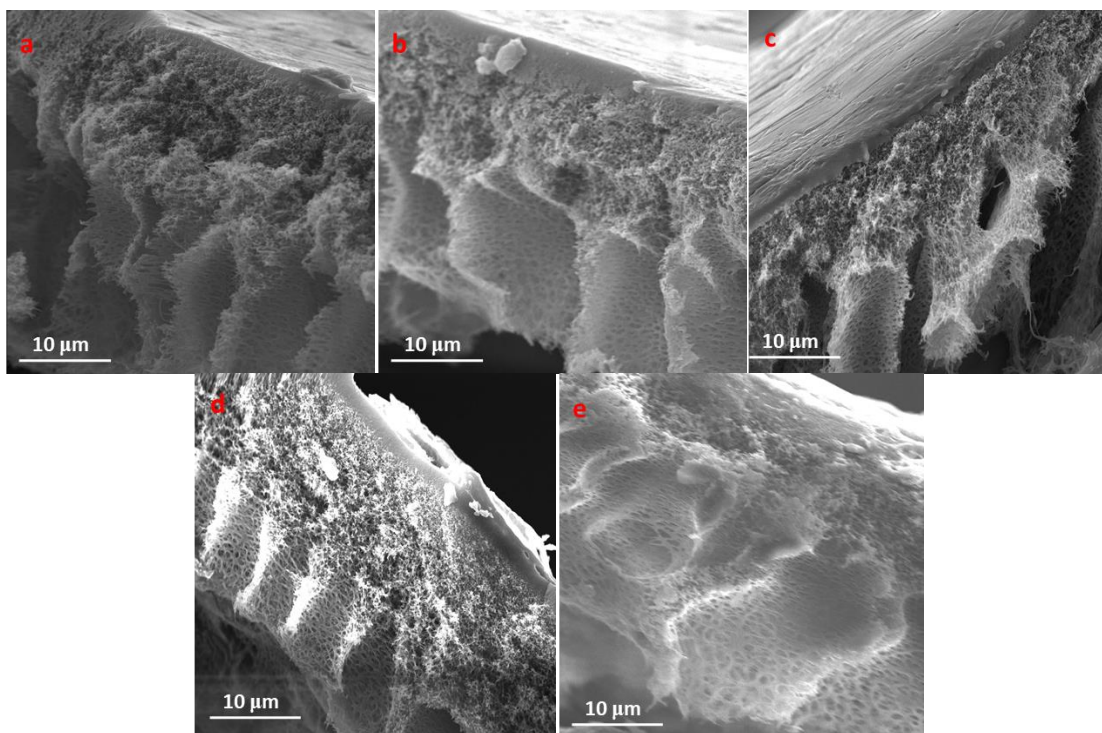
Fig. 3. Cross-sectional SEM images of (a) pristine PSf, (b) 1% HPEI/PSf, (c) 2% HPEI/PSf, (d) 3% HPEI/PSf, and (e) 4% HPEI/PSf membranes.

bands for the polysulfone, which showed peaks at 1550 cm^{-1}, 3350 cm^{-1} and 2843 cm^{-1}, were ascribed to -SO$_2$, -OH and -CH stretching bands, respectively. Figure 1 (b) illustrates an expanded view of the amide functional region. New absorption bands of the various HPEI loadings on the PSf membranes were observed at 1576 cm^{-1}, 1641 cm^{-1} and 1722 cm^{-1}, which correspond to the respective amide-II (-CONH-), amide-I [(bending vibrations of the -N-H bond in (-CONH-)] and C=O stretching bands of the carboxylic acid group (-COOH) [20, 26]. The latter absorption band resulted from the hydrolysis of the acyl chloride group (-COCl) of the TMC [29]. These results demonstrate that the membranes are a composite of two precursor polymers, namely PSf and HPEI. Therefore, FTIR-ATR spectral analysis provides evidence for the successful modification of the PSf membrane with HPEI.

3.2. SEM Analysis

SEM images (see Figure 2) illustrate the morphological changes of the pristine and modified membranes at 3000 x magnification. The pristine PSf membrane, which is shown in Figure 2 (a), displayed a smooth, featureless and unstructured morphology. Upon interfacial polymerization of HPEI with the PSf substrate, a rougher surface was observed (see Figure 2 (b-e)) [35, 36]. Thus, the interfacial polymerization between HPEI and TMC generated a relatively dense selective layer on the PSf support membrane, which, (as illustrated in in Figure 2 (b-e), clearly indicates the depositions of the HPEI polymer. The HPEI polymer and TMC react by both inter and intra-molecular processes, which may have resulted in the congregation of HPEI molecules on the surface of the membrane thus forming the depositions on the membrane surface [37].
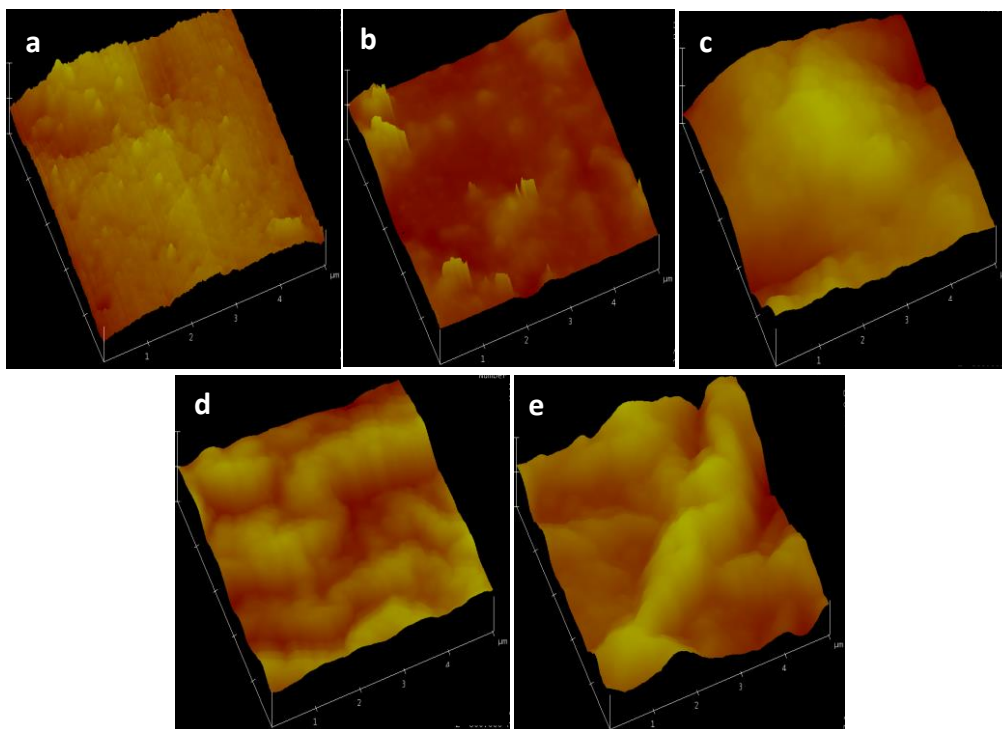
Fig. 4. Three-dimensional AFM images of (a) pristine PSf, (b) 1% HPEI/PSf, (c) 2% HPEI/PSf, (d) 3% HPEI/PSf, and (e) 4% HPEI/PSf membranes.

The cross-sectional view (see Figure 3) of the membranes revealed their asymmetric nature following the deposition of a polyamide thin film. In Figure 3 (a) the pristine PSf membrane can be seen displaying a sponge-like morphology. Whereas the HPEI modified membranes (see Figure 3 (b-e)) displayed finger-like morphology on the membrane surface. Upon deposition of the polyamide thin film, the pore sizes of the modified membranes were decreased [34]. This could be attributed to partial pore blockage during the formation of the TFC membrane. When the loading of HPEI was increased, the polyamide skin layer became noticeably thicker. The thicker skin layer subsequently increases the thickness of the pore walls which leads to higher tortuosity [38]. The sponge-like morphology of the pristine PSf membrane resulted in higher permeation of water molecules through the membrane, which endowed it with a higher water flux. Hence, the pristine membrane's porous structure usually reduces the transmembrane resistance to water flow, allowing the passage of water molecules through the membrane [21].

3.3. Atomic Force Microscopy

AFM analysis was implemented to compare the surface topographies of the pristine and HPEI modified membranes. Figure 4 illustrates the rougher surfaces generated for all the interfacial polymerized membranes (see Figure 4 (b-e)] compared to the pristine PSf membrane (see Figure 4 (a)). The observed nodules are bright high peaks whereas the pores are seen as dark depressions.

The statistical roughness information in terms of surface roughness (R_q) and mean surface roughness (R_a) are given in Table 1. The surface roughness of the membranes ranged from 13.9 nm for the pristine PSf membrane (see Figure 4 (a)) to 140.0 nm for the 4% HPEI/PSf modified membranes (see Figure 4 (e)). The abundant amine groups on HPEI essentially act as hydrogen chloride scavengers during the polycondensation reaction between HPEI and TMC [35]. During this reaction, more polyamide functional groups and hydrogen chloride compounds are generated, thereby altering the surfaces of the membranes. These results correspond with the SEM analysis (see Figure 2 (a-e)) where the morphology transgressed from smooth featureless to a denser and rough surface following modification with HPEI. Furthermore, the change in surface roughness parameters was found to be proportional to the pore size of the membranes [39]. This trend can be explained by the creation of deep depressions (i.e., pores) and large nodules during the formation of the polyamide thin film at high HPEI concentrations [40]. These large nodules can result in the constriction of the pores as shown in this study.

Table 1
AFM statistical data.

Membrane	Surface roughness (R_q) (nm)	Mean surface roughness (R_a) (nm)
Pristine PSf	13.9	11.2
1% HPEI/PSf	41.6	30.4
2% HPEI/PSf	93.1	78.0
3% HPEI/PSf	95.5	80.6
4% HPEI/PSf	140.0	117.5

3.4. Membrane water permeation studies

The pure water flux of the membranes was investigated (see Figure 5) and an increase in pure water flux with an increase in pressure was observed for all membranes. The pristine PSf membrane showed the highest water permeation, which was consistent with its large pore size. This observation was complemented by its sponge-like morphology, as shown in Figure 3 (a), which provided easy passage of water molecules. On the other hand, the modified membranes generally exhibited lower pure water flux which could be assigned to the formation of a polyamide layer on the surface of the membranes. As the HPEI loading increased, the pure water flux of the modified membranes decreased (for example, 78.40 L·m^{-2}·h^{-1} for 3% HPEI to 48.32 L·m^{-2}·h^{-1} for 4% HPEI operated at 600 kPa). The high pure water flux for the 3% loading could be ascribed to a pronounced swollen network structure, effectively being able to attract water molecules within the membrane pores as well as being attracted via hydrogen bonding from peripheral amine groups.

Table 2 shows the membrane properties of the pristine and modified membranes, including the contact angle, water uptake capacity, porosity, pore size and the film thickness. As the concentration of HPEI increased, there was a noticeable decrease in contact angle from 76.31° to 69.04° for the 1% HPEI/PSf and 4% HPEI/PSf modified membranes, respectively. This decrease in contact angle can be ascribed to an increase in the effective surface area of HPEI, thereby allowing water molecules to interact with terminal amine functional groups. As the HPEI content was increased this resulted in an increase in the abundance of amine functional groups on the membranes surface. The presence of the abundant amine functional groups enhanced the hydrophilicity of the membranes. Sun et al. reported similar

findings where the increase in HPEI resulted in more amine groups being attached to the membrane surface of the polyamide-imide hollow fiber membrane surface [41]. It is for this reason why an increase in the hydrophilicity was observed. Since both the C-N and N-H bonds in HPEI are polar due to the electronegativity of the nitrogen atoms, the HPEI modified membranes provide high polarity to the membrane surface, which attracts polar molecules such as water. Thus, modification with HPEI introduced more sites for hydrogen bonding to occur. These observations showed that the introduction of HPEI could effectively enhance the hydrophilicity of the PSf membranes. It is widely known that the hydrophilicity is directly proportional to the contact angle. Whereas, both the hydrophilicity and the contact angle measure the membrane surface, the pure water flux is largely dependent on the bulk properties such as membrane thickness, porosity and pore size [42]. The polyamide layer on the membrane resulted in a decrease in the pore size, hence the pure water flux decreased.
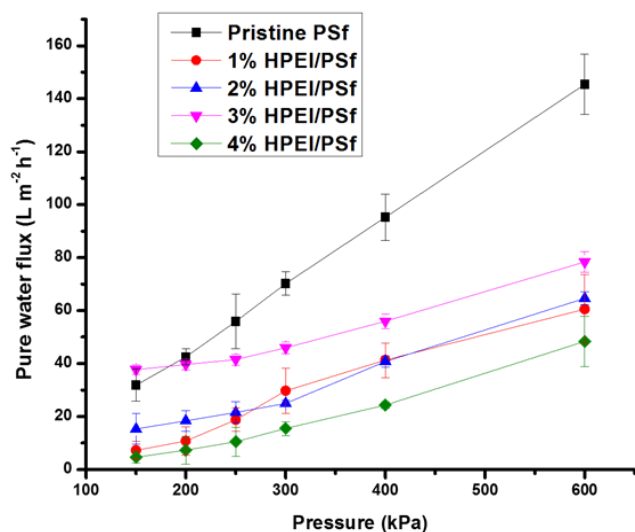

Fig. 5. Pure water flux versus transmembrane pressure.

The contact angle of the 2% HPEI/PSf membrane was the lowest (39.97°) because the HPEI was uniformly distributed on the membrane. Consequently, the water molecules could efficiently react with the abundant amine groups of HPEI due to the decreased surface energy of the 2% HPEI/PSf membrane [35]. However, the contact angle was observed to slightly increase at higher HPEI loadings (i.e. 3% and 4%). This increase can be ascribed to the agglomeration of the HPEI as it is increased [43]. At increased HPEI loading (>3% HPEI/PSf), it is possible that during the drying process the -NH$_2$ and -COOH functional groups swing inside the polymer chain network [44]. Correspondingly, a conformational transformation occurs between the internal hydrophobic core and the external hydrophilic surface layer, where the hydrophobic cavities of HPEI could migrate to the surface of the membrane [39, 44, 45]. It is noteworthy that even though the contact angle measurements of the highly loaded HPEI/PSf membranes were increasing, they still exhibited lower values compared to the pristine PSf membrane. These results indicate that the modification of PSf with HPEI significantly enhances the hydrophilicity of the membranes.

Table 2
Contact angle and porosity measurements for pristine and HPEI modified membrane.

Membrane	Contact angle (°)	Water uptake capacity (%)	Porosity (%)	Thickness (µm)	Pore size (µm)
Pristine PSf	86.95	53.5±0.7	71.22	155.71±2.8	0.283
1% HPEI/PSf	76.31	93.6±0.37	40.14	169.22±4.1	0.133
2% HPEI/PSf	39.97	96.6±0.76	42.52	174.52±3.6	0.121
3% HPEI/PSf	63.64	87.4±0.51	47.37	182.67±5.3	0.112
4% HPEI/PSf	69.04	75.1±0.7	53.43	191.62±2.7	0.194

The water-uptake capacity (see Table 2) increased after interfacial polymerization of PSf with HPEI. This observation could be due to the enhanced hydrophilicity as well as the degree of crosslinking during polymerization as the concentration of HPEI increased. Generally, when the thin film composite layer of the modified membrane is not completely crosslinked, there will still be free NH$_2$ groups, as observed in Figure 1 (b), where primary amine absorption bands can be seen at 1576 cm^{-1} after HPEI modification. It is thus important to only do a partial crosslinking (~0.2% TMC) to leave free NH$_2$ groups for hydrogen bonding with water molecules [46]. In addition, unreacted acyl chloride functional groups from TMC can form carboxylic acid groups once reacted with moisture as illustrated in the FTIR spectrum (see Figure 1 (b)). The presence of -COOH functional groups not only enhances hydrophilicity but also improves water uptake.

The thickness of the selective layer was measured using ImageJ software from the cross sectional SEM images [24, 47]. The thickness of the modified membranes increased as the HPEI loading increased, as shown in Table 2. The increased resistance to the flow of water molecules through the membrane is linked to the increase in the active layer thickness. It has also been observed that the crystalline nature of a polyamide thin film hinders polymer chain movements which subsequently influences interaction with water molecules upon an increase in film thickness [48]. Furthermore, the more TMC crosslinking points there were, i.e. higher concentration of HPEI, the denser the active crosslinked active layer was. Wei and co-workers obtained similar results where a nanofiltration membrane was developed from hydroxyl-ended polyester and TMC using PSf as support. The results obtained by this team indicated that a crosslinked hyperbranched polyester produced a uniform, ultra-thin active layer on top of a PSf membrane support. Moreover, in this study, the pure water flux was observed to decrease as the HPEI content increases. This led to more HPEI molecules being adsorbed onto the surface of the PSf membrane resulting in a denser top layer, thus reducing the water flux of the modified membranes [49]. These observations agreed with the cross-sectional images obtained from SEM (see Figure 3 (b-e)) where the deposition of an active layer has been formed on the surface of the PSf membrane. This increase in thickness was due to the increase in HPEI loadings which produced denser layers on the membranes when compared to the pristine membrane.

The porosity and pore size of the membranes decreases upon increased HPEI loading for all modified membranes. The 2% and 3% HPEI/PSf membranes had the lowest pore size (i.e., 0.113 and 0.102 µm, respectively) as compared to the pristine PSf and other modified membranes as shown in Table 2. The narrow pore size of the aforementioned membranes indicated full saturation of the PSf membrane pores with the HPEI polymer. This decrease in pore size and porosity illustrates a reduction in the number of pores per unit area after modification with HPEI. Moreover, the trend observed in membrane porosity may also be partially caused by the generation of thicker pore walls as HPEI content increased [38]. Fang et al. reported similar findings where the increase in HPEI content caused a gradual decrease in the pore size in a polyethersulfone/polyvinylpyrrolidone (PES/PVP) membrane. The authors ascribed the decrease in average pore size to the leaching of HPEI from PVP in the casting solution. Moreover, at higher HPEI loadings, the solution's viscosity increased which hindered pore formation [25]. Increasing the HPEI loading, may have led to the formation of pores during the sulfone-amine bond formation. In this case, pores are reformed due to the creation of open spaces at high polymer loadings i.e. 4% HPEI/PSf.

3.5. Streaming potential analysis

To accurately confirm the mechanism of As(III) removal, zeta potential studies were conducted. In these experiments, the zeta potential was determined at the solid/liquid interface of macroscopic surfaces based on the measurement of streaming potential and streaming current, respectively. The zeta potential of the membrane is determined by the moieties on the surface of the membranes since it is measured in relation to the streaming potential. Figure 6 illustrates the obtained zeta potential results. In acidic pHs the zeta potential was mainly positive for all membranes. However, when operating at highly alkaline conditions (above pH=10), the zeta potential drastically decreased towards the negative range. It has been reported that in some cases the outermost surface of the polyamide thin film layer is rich in carboxylic acid groups which originates from hydrolysis of TMC as compared to the rest of the layer which is rich in amine groups [50]. At highly alkaline pH, the carboxylic acid groups are deprotonated leading to negatively charged ions. In contrast, at low pH values, protonation of the amine groups occurs thereby generating a higher positive charge on the probed surface of the membranes. At the operating pH of this study (pH=9.4) the HPEI/PSf membranes were positively charged, whereas the As(III) exists as negative species. Thus it is suggested that the As(III) removal could be attributed to adsorption via the

attraction of opposite charged species for the HPEI modified membranes and charge repulsion (Donnan exclusion) for the pristine PSf membrane.
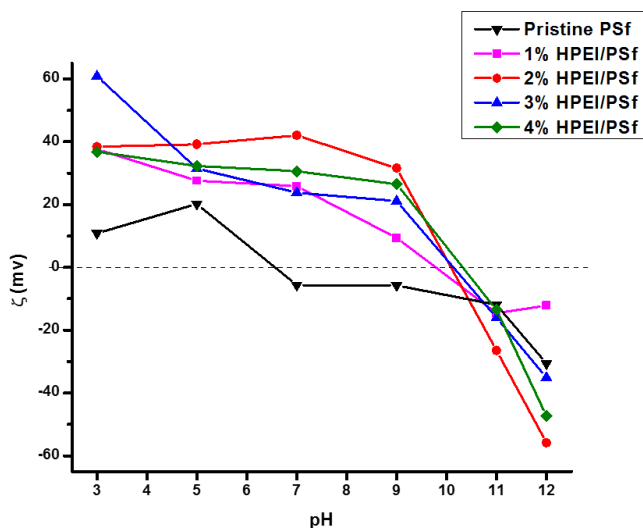
4. Rejection studies

The ability of the modified membranes to remove As(III) was investigated using synthetic and spiked tap water samples. Figure 7 (a) shows that over 120 minutes the rejection of As(III) in synthetic water increased to 20%, 58%, 78%, 60% and 58% for pristine PSf, 1%, 2%, 3% and 4% HPEI/PSf membranes, respectively. Figure 7 (b), which show the results obtained for the spiked tap water samples, indicate that the removal of As(III) increased after 120 min to 1%, 13%, 55%, 60% and 25% for pristine PSf, 1%, 2%, 3% and 4% HPEI/PSf membranes, respectively. Three possible mechanisms for the rejection of As(III) are proposed: 1) electrostatic repulsion of similarly charged species, 2) adsorption of the positively charged HPEI molecule and the negatively charged As(III), and lastly 3) size exclusion based on the difference in pore size and the size of As(III) ions.

The first rejection mechanism can occur via electrostatic repulsion where two similarly charged species repel each other. The electrostatic repulsion mechanism occurs at high pH values (pH=11) where both the pristine membrane and the HPEI modified membranes are negatively charged. At pH 11, As(III) is negatively charged, thereby being repelled by the pristine and HPEI/PSf membranes. The pH effects of the membranes on As(III) removal in synthetic water was also studied and is shown in Figure 8. The general rejection mechanism can be seen in Figure 9. In general, under acidic conditions, fewer As(III) were removed as compared to studies done at alkaline pHs.
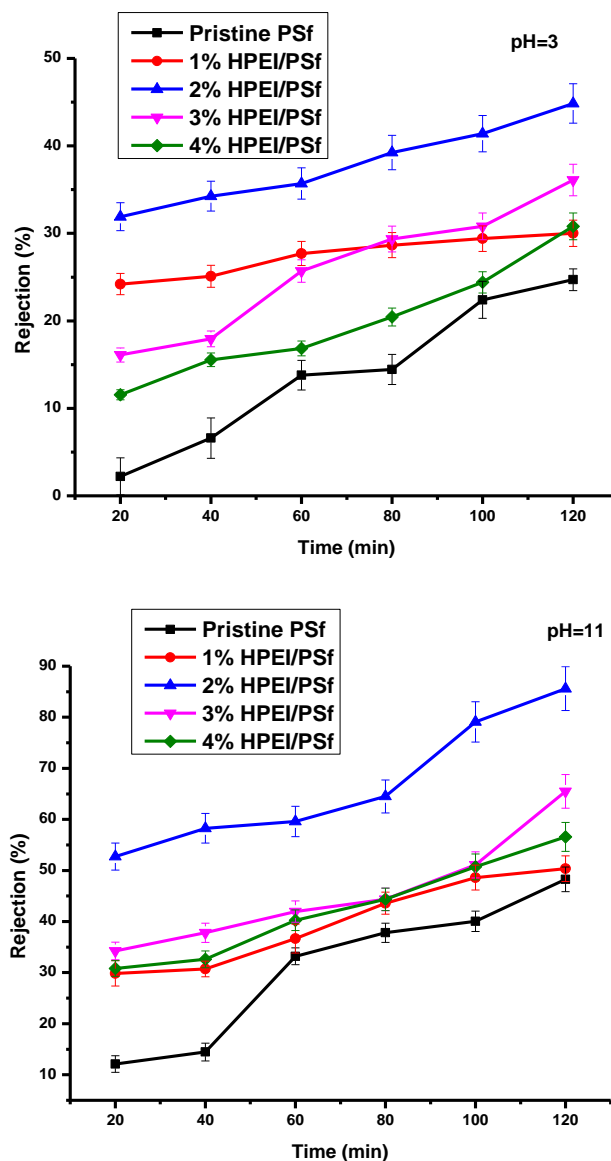

Fig. 6. Zeta potential (ξ) of pristine and HPEI modified membranes.

Fig. 7. As(III) rejection from (a) synthetic and (b) spiked tap water.

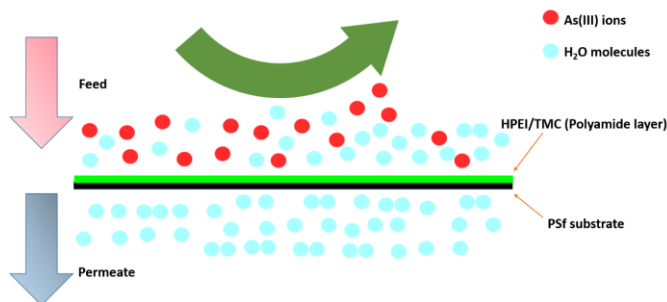**Fig. 8.** pH effects on As(III) removal in synthetic water.

Fig. 9. As(III) electrostatic repulsion rejection scheme.

The second proposed mechanism of As(III) rejection was understood to be due to electrostatic attraction, i.e. adsorption. In this rejection mechanism species of opposite charges are attracted to one another via coulombic interactions. With reference to the zeta potential studies (see Figure 6), the predominant rejection mechanism at pH 9.4 was ascribed to adsorption. At the operating pH of 9.4 in this study, coulombic interactions occur between the positively charged HPEI modified membrane and the negatively charged As(III) ions [44]. This process is driven mainly by Van der Waals forces and electrostatic forces between the adsorbate ions [As(III)] and the adsorbent surface molecules (HPEI) [51]. In addition to adsorption, metal ions can also be trapped in the nanocavities of the HPEI polymer, thereby illustrating its multifunctionality in water applications. Therefore, even though arsenic ions may pass through the membranes, it will be trapped/chelated with the lone pairs on internal nitrogen atoms from HPEI forming a complex, thus removing As(III) from water [13, 52]. Fewer As(III) ions could be chelated onto the HPEI/PSf membranes in tap water samples (see Figure 7 (b)) due to a lack of active sites. Yoo and co-workers obtained comparable results where they used a hyperbranched poly(amidoamine) (HPAMAM)-grafted poly(tetrafluoroethylene) (PTFE) microfiltration membrane for the removal of Cu(II). The resulting microfiltration membranes were found to adsorb 72% of Cu^{2+} ions. The mechanism of rejection as stated by the authors was due to the positively charged heavy metal ions which could be adsorbed via electrostatic interactions with negatively charged matrices, or via the donation of lone-pair electrons of the matrix to metal ions to form coordinate bonds [27].

Generally, as the concentration of the HPEI increases, a higher As(III) rejection was observed (see Figure 7 (a) and (b)). The rejection of As(III) in synthetic solutions was observed to be higher than that of tap water. This higher rejection was accredited to the difference in matrices of the two solutions. In tap water there are various alkali and alkali earth metals including Na^+, Ca^{2+} and Mg^{2+} present with As(III) [53]. The matrix present in tap water samples may severely affect the transport of water and rejection of As(III) since the multi-metal matrix possibly competed with As(III) for active sites within HPEI's core for complexation [29, 30].

The last mechanism of rejection may be due to size exclusion, where particles may sieve through the membrane due to its varied pore sizes. Hence, the negligible rejection of the pristine PSf membrane towards As(III) may be due to its large pore size. This phenomenon is emphasized in the tap water samples (see Figure 7 (b)). The atomic radius of As(III) (i.e., 114 pm) is much lower than that of magnesium (i.e., 145 pm) and calcium (i.e., 194 pm). As a result, the pristine membrane could have sieved the latter metals due to their larger atomic radii and allowed As(III) to penetrate through its pores. Heffron and co-workers obtained relatable results, where lower removal of certain heavy metals was observed in simulated water which contained arsenic, chromium and nickel metals. The removal via electro-coagulation of individual metals was observed to be much higher than that of a mixed matrix [54].

Figure 10 (a) and (b) illustrate the permeate flux of the membranes. As could be observed, at a transmembrane pressure of 600 kPa, the permeate flux decreased over time for all the membranes. Generally, the retention of the membrane depends on the structure of the top/active layer and rarely depends on the structure of the membrane sub-layers [55]. As the filtration time increased, there could be a build-up of As(III) ions on the surface of the membranes and within the membranes matrix which might cause partial blockage of the membrane pores. The increase in membrane thickness after rejection could also lead to an increase in the path length across the membranes hence causing resistance to the flow of water through the membrane. Furthermore, the interconnectivity of the sulfonated-amine (PSf-HPEI) macrodomains is likely to be enhanced with an increase in HPEI concentration, thereby promoting the transport of water and restriction of

arsenic through the membrane [56]. This could explain why the permeate flux of the 2% and 3% HPEI loadings was the highest of the HPEI modified membranes. The permeate flux of tap water samples generally remained constant throughout the filtration procedure as shown in Figure 10 (b) apart from the pristine PSf membrane which displayed the highest permeate flux. In these spiked tap water samples, the permeate flux was dramatically lower than the synthetic samples for the HPEI modified membranes. This decreased flux was attributed to the complex matrix found in tap water. In contrast, the pristine PSf membrane showed the highest permeate flux for both tested water samples. This can be explained by its open network structure. Therefore, As(III) (and possibly other metal ions in tap water) could permeate through the pores of the pristine PSf membrane without any great difficulty.
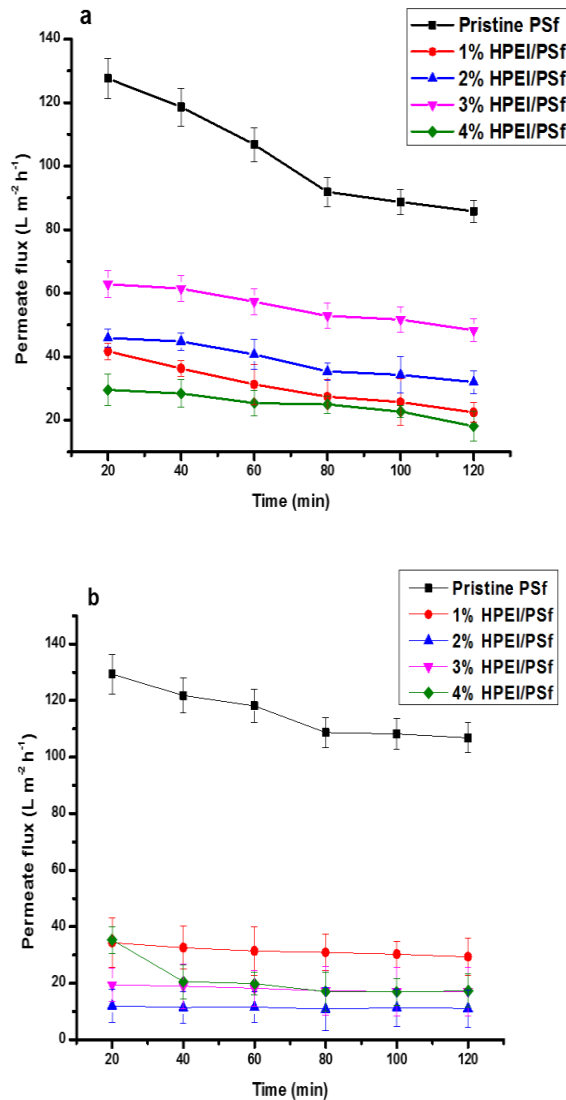

Fig. 10. As(III) permeate flux of (a) synthetic and (b) spiked tap water.

5. Conclusions

The current study demonstrates the fabrication and application of an interfacial polymerized thin film composite HPEI/PSf membrane for the removal of As(III) from synthetic and spiked tap water solutions. Zeta potential studies confirmed that the predominant method of rejection occurred via adsorption. The synthesized membranes of polyamide origin could decrease the As(III) concentration by 78% (synthetic water) for the 2% HPEI/PSf membrane, whereas the 3% HPEI/PSf membrane rejected 60% in spiked tap water samples after 2 hours. The composite HPEI/PSf membranes showed an increase in hydrophilicity where the highest degree of hydrophilicity was observed for the 2% HPEI/PSf membrane (39.97°) compared to the pristine PSf membrane (86.95°). Water permeation studies

illustrated that the selectivity and permeability can systematically be enhanced by simply optimizing the HPEI content. The trend observed was that the 2% and 3% HPEI/PSf membranes were the optimum loadings in terms of membrane performance (i.e., permeation and rejection). Therefore, hyperbranched polymers modified membranes show promising results in the removal of As(III) in both synthetic and spiked tap water samples and has potential to be used in large-scale water remediation processes.

6. Acknowledgments

References

[1] H. Salazar, J. Nunes-Pereira, D. M. Correia, V. F. Cardoso, R. Gonçalves, P. M. Martins, S. Ferdov, M. D. Martins, G. Botelho, S. Lanceros-Méndez, Poly(vinylidene fluoride-hexafluoropropylene)/bayerite composite membranes for efficient arsenic removal from water, Mater. Chem. Phys. 183 (2016) 1–9.

[2] M. R. Ramudzuli,A. C. Horn, Arsenic residues in soil at cattle dip tanks in the Vhembe district, Limpopo Province, South Africa, S. Afri. J. Sci. 110 (2014) 1–7.

[3] SANS, Drinking water Quality Requirements: South African National Standard 241: drinking water (ed. 6). South Africa, Pretoria, 2006 (2006) 6–8.

[4] P. Kempster, M. Silberbauer, A. Kuhn, Interpretation of drinking water quality guidelines – The case of arsenic, Water SA. 3 (2007) 95–100.

[5] K. Sami and A. Druzynski, Predicted spatial distribution of naturally occurring arsenic, selenium and uranium in groundwater in South Africa, WRC report no. 1236/1/03. 2003.

[6] M. Cakmakci, A. B. Baspinar, U. Balaban, V. Uyak, I. Koyuncu, C. Kinaci, Comparison of nanofiltration and adsorption techniques to remove arsenic from drinking water, Desalin. Water Treat. 9 (2009) 149–154.

[7] C. Trois, A. Cibati, South African sands as an alternative to zero valent iron for arsenic removal from an industrial effluent: batch experiments, J. Environ. Chem. Engi. 3 (2015) 488–498.

[8] W. J. Lau, S. Gray, T. Matsuura, D. Emadzadeh, J. Paul Chen, and A. F. Ismail, A review on polyamide thin film nanocomposite (TFN) membranes: History, applications, challenges and approaches, Water Res. 80 (2015) 306–32.

[9] E. Erhan, B. Keskinler, G. Akay, O. F. Algur, Removal of phenol from water by membrane-immobilized enzymes: Part I. Dead-end filtration, J. Membr. Sci. 206 (2002) 361–373.

[10] M. M. Mahlambi, Polymerization of cyclodextrin-ionic liquid complexes for the removal of organic and inorganic contaminants from water, University of Johannesburg, South Africa, 2007.

[11] J. Lin, W, Ye, H. Zeng, H. Yang, J. Shen, S. Darvishmanesh, P. Luis, A. Sotto, B. Van Der Bruggen, Fractionation of direct dyes and salts in aqueous solution using loose nanofiltration membranes, J. Membr. Sci. 477 (2015) 183–193.

[12] J. Lin, C. Y. Tang, W. Ye, S. Sun, S. H. Hamdan, A. Volodin, C. Van Haesendonck, A. Sotto, P. Luis, and B. Van Der Bruggen, Unraveling flux behavior of superhydrophilic loose nanofiltration membranes during textile wastewater treatment, J. Membr. Sci. 493 (2015) 690–702.

[13] J. Lin, W. Ye, J. Huang, B. Ricard, M. Baltaru, B. Greydanus, S. Balta, J. Shen, M. Vlad, A. Sotto, P. Luis, and B. Van Der Bruggen, Toward resource recovery from textile wastewater: dye extraction, water and base/acid regeneration using a hybrid NF-BMED process, Sustain. Chem. Eng. 3 (2015) 1993–2001.

[14] J. Lin, C. Y. Tang, C. Huang, Y. Pan, W. Ye, J. Li, J. Shen, R. Van Den Broeck, J. Van Impe, A. Volodin, C. Van Haesendonck, A. Sotto, P. Luis, B. Van Der Bruggen, A comprehensive physico-chemical characterization of superhydrophilic loose nanofiltration membranes, J. Membr. Sci. 501 (2016) 1–14.

[15] V. Vatanpour, S. S. Madaeni, S. Zinadini, H. R. Rajabi, Development of ion imprinted technique for designing nickel ion selective membrane, J. Membr. Sci. 373 (2011) 36–42.

[16] L. C. Koh, W. Y. Ahn, M. M. Clark, Selective adsorption of natural organic foulants by polysulfone colloids: Effect on ultrafiltration fouling, J. Membr. Sci. 281 *(*2006*)* 472–479.

[17] N. Hu, J. Y. Yin, Q. Tang, Y. Chen, Comparative study of amphiphilic hyperbranched and linear polymer stabilized organo-soluble gold nanoparticles as efficient recyclable catalysts in the biphasic reduction of 4-nitrophenol, J. Polym. Sci. A. 49 (2011) 3826–3834.

[18] M. R. Kotte, M. Cho, M. S. Diallo, A facile route to the preparation of mixed matrix polyvinylidene fluoride membranes with in-situ generated polyethyleneimine particles, J. Membr. Sci. 450 (2014) 93–102.

[19] C. Zhou, Y. Shi, C. Sun, S. Yu, M. Liu, Thin film composite membranes formed by interfacial polymerization with natural material sericin and trimesoyl chloride for nanofiltration, J. Membr. Sci. 471 (2014) 381–391.

[20] M. Seiler, "Hyperbranched polymers: Phase behaviour and new applications in the field of chemical engineering, Fluid Phase Equilib. 241 (2006) 155–174.

[21] K. N. Han, B. Y. Yu, S. Y. Kwak, Hyperbranched poly(amidoamine)/polysulfone composite membranes for Cd(II) removal from water, J. Membr. Sci. 396 (2012) 83–91.

[22] D. M. Saad, E. M. Cukrowska, H. Tutu, Functionalisation of cross-linked polyethylenimine for the removal of As from mining wastewater, Water SA, 39

(2013) 257–264.

[23] W. Huang, J. N. Kuhn, C. K. Tsung, Y. Zhang, S. E. Habas, P. Yang, G. A. Somorjai, Dendrimer templated synthesis of one nanometer Rh and Pt particles supported on mesoporous silica: catalytic activity for ethylene and pyrrole hydrogenation, Nano Lett. 8 (2008) 2027–2034.

[24] S. J. Park, R. K. Cheedrala, M. S. Diallo, C. Kim, I. S. Kim, W. A. Goddard, Nanofiltration membranes based on polyvinylidene fluoride nanofibrous scaffolds and crosslinked polyethyleneimine networks, J. Nano Part. Res.14 (2014) 33–46.

[25] X. Fang, J. Li, X. Li, X. Sun, J. Shen, W. Han, L. Wang, Polyethyleneimine, an effective additive for polyethersulfone ultrafiltration membrane with enhanced permeability and selectivity, J. Membr. Sci. 476 (2015) 216–223.

[26] D. Qu, J. Wang, D. Hou, Z. Luan, B. Fan, and C. Zhao, Experimental study of arsenic removal by direct contact membrane distillation, J. Hazard. Mater. 163 (2009) 874–879.

[27] H. Yoo, S. Kwak, Surface functionalization of PTFE membranes with hyperbranched poly(amidoamine) for the removal of Cu^{2+} ions from aqueous solution, J. Membr. Sci. 448 (2013) 125–134.

[28] T. Hong, A. Ngo, T. Xuan, D. T. Tran, T. Xuan, Removal of heavy metal ions in water using modified polyamide thin film composite, Int. J. Sci. Technol. 3 (2017) 91–103.

[29] D. Wu, Y. Huang, S. Yu, D. Lawless, X. Feng, Thin film composite nanofiltration membranes assembled layer-by-layer via interfacial polymerization from polyethylenimine and trimesoyl chloride, J. Membr. Sci. 472 (2014) 141–153.

[30] J. Zhu, Q. Zhang, S. Li, S. Zhang, Fabrication of thin film composite nanofiltration membranes by coating water soluble disulfonated poly(arylene ether sulfone) and in situ crosslinking, Desalination, 387 (2016) 25–34.

[31] X. Zhao, J. Ma, Z. Wang, G. Wen, J. Jiang, F. Shi, L. Sheng, Hyperbranched-polymer functionalized multi-walled carbon nanotubes for poly(vinylidene fluoride) membranes: from dispersion to blended fouling-control membrane, Desalination, 303, (2012) 29–38.

[32] C. Liao, J. Zhao, P. Yu, H. Tong, Y. Luo, Synthesis and characterization of low content of different SiO₂ materials composite poly(vinylidene fluoride) ultrafiltration membranes, Desalination, 285 (2012) 117–122.

[33] L. Wang, S. Ji, N. Wang, R. Zhang, G. Zhang, J. Li, One-step self-assembly fabrication of amphiphilic hyperbranched polymer composite membrane from aqueous emulsion for dye desalination, J. Membr. Sci. 452 (2014) 143–151.

[34] D. Zhao, Y. Yu, J. P. Chen, Zirconium/polyvinyl alcohol modified flat-sheet polyvinylidene fluoride membrane for decontamination of arsenic: Material design and optimization, study of mechanisms, and application prospects, Chemosphere 155 (2016) 630–639.

[35] B. Rajaeian, A. Rahimpour, M. O. Tade, S. Liu, Fabrication and characterization of polyamide thin film nanocomposite (TFN) nanofiltration membrane impregnated with TiO₂ nanoparticles, Desalination, 313 (2013) 176–188.

[36] H. S. Lee, S. J. Im, J. H. Kim, H. J. Kim, J. P. Kim, B. R. Min, Polyamide thin-film nanofiltration membranes containing TiO₂ nanoparticles, Desalination, 219 (2008) 48–56.

[37] S.P. Malinga, O.A. Arotiba, R. W. M. Krause, S.F. Mapolie, M.S. Diallo, BB. Mamba. Cyclodextrin-dendrimer functionalized polysulfone membrane for the removal of humic acid in water. J. Appl. Polym. Sci. 130 (2013) 4428-4439.

[38] Z. X. Low, Q. Liu, E. Shamsaei, X. Zhang, H. Wang, Preparation and characterization of thin-film composite membrane with nanowire-modified support for forward osmosis process, Membranes, 5 (2015) 136–149.

[39] S. P. Malinga , O. A. Arotiba , R. W. M. Krause , S. F. Mapolie , M. S. Diallo and B. B. Mamba. Nanostructured β-cyclodextrin-hyperbranched polyethyleneimine (β-CD-HPEI) embedded in polysulfone membrane for the removal of humic acid from Water, Sep. Sci. Technol. 48 (2013) 2724-2734.

[40] S. Simone, F. Galiano, M. Faccini, M. E. Boerrigter, C. Chaumette, E. Drioli, A. Figoli, Preparation and characterization of polymeric-hybrid PES/TiO₂ hollow fiber membranes for potential applications in water treatment, Fibers, 5 (2017) 1-19.

[41] S. P. Sun, T. A. Hatton, T. S. Chung, Hyperbranched polyethyleneimine induced cross-linking of polyamide-imide nanofiltration hollow fiber membranes for effective removal of ciprofloxacin, Environ. Sci. Technol. 45 (2011) 4003–4009.

[42] A. Schulze, M. Went, and A. Prager, Membrane functionalization with hyperbranched polymers, Materials, 9 (2016) 1-11.

[43] K. E-sik and B. Deng. Fabrication of polyamide thin-film nano-composite (PA-TFN) membrane with hydrophilized ordered mesoporous carbon (H-OMC) for water purification. J. Membr. Sci. 375 (2011) 46-54.

[44] Y. C. Chiang, Y. Z. Hsub, R. C. Ruaan, C. J. Chuang, K. L. Tung, Nanofiltration membranes synthesized from hyperbranched polyethyleneimine, J. Membr. Sci. 326 (2009) 19–26.

[45] H. Wang, N. Shao, S. Qiao, and Y. Cheng, Host–guest chemistry of dendrimer–cyclodextrin conjugates: selective encapsulations of guests within dendrimer or cyclodextrin cavities revealed by NOE NMR techniques, J. Phys. Chem. B 116 (2012) 11217–11224.

[46] M. Obaid, O. A. Fadali, B. H. Lim, H. Fouad, N. A. M. Barakat, Super-hydrophilic and highly stable in oils polyamide-polysulfone composite membrane by electrospinning, Mater. Lett. 138 (2015) 196–199.

[47] M. D. Abràmoff, P. J. Magalhães, S. J. Ram, Image processing with ImageJ, J. Biophotonics Int. 11 (2003) 36–41.

[48] B. S. Mbuli, S. D. Mhlanga, B. B. Mamba, E. N. Nxumalo, Fouling resistance and physicochemical properties of polyamide thin-Film composite membranes modified with functionalized cyclodextrins, Adv. Polym. Tech. 36 (2016) 249-260.

[49] X. Z. Wei, L. P. Zhu, H. Y. Deng, Y. Y. Xu, B. K. Zhu, Z. M. Huang, New type of nanofiltration membrane based on crosslinked hyperbranched polymers, J. Membr. Sci. 323 (2008) 278–287.

[50] M. Dalwani, Thin film composite nanofiltration membranes for extreme conditions, University of Twente, Netherlands, 2011.

[51] N. R. Nicomel, K. Leus, K. Folens, P. Van Der Voort, G. Du Laing, Technologies

for arsenic removal from water: current status and future perspectives, Int. J. Environ. Res. Public. Health. 13 (2015) 1–24.

[52] J. Song, M. Zhang, A. Figoli, Y. Yin, B. Zhao, X. M. Li, and T. He, Arsenic removal using a sulfonated poly(ether ether ketone) coated hollow fiber nanofiltration membrane, Environ. Sci. Water Res.Technol. 1 (2015) 839–845.

[53] P. Shah, C. N. Murthy, Studies on the porosity control of MWCNT/polysulfone composite membrane and its effect on metal removal, J. Membr. Sci. 437 (2013) 90–98.

[54] J. Heffron, M. Marhefke, B. K. Mayer, Removal of trace metal contaminants from potable water by electrocoagulation, Scientific Reports, 6 (2016) 1–9.

[55] E. Saljoughi, S. M. Mousavi, Preparation and characterization of novel polysulfone nanofiltration membranes for removal of cadmium from contaminated water, Sep. Sci. Technol. 90 (2012) 22–30.

[56] Z. Thong, G. Han, Y. Cui, J. Gao, T. S. Chung, S. Y. Chan, S. Wei, Novel nanofiltration membranes consisting of a sulfonated pentablock copolymer rejection layer for heavy metal removal, Environ. Sci. Technol. 48 (2014) 13880–13887,